Supporting Information

Organic Ammonium Flexibility Modulated Phase-Transition Behaviour in 3D Perovskite-like Mixed-valence Iron Complexes

Experimental section

Materials

All chemicals were reagent grade and used as purchased without further purification.

Synthesis

$[HPy]_2[Fe^{III}Fe^{II}_2(HCOO)_7(C_2O_4)]$ (**1**): 0.10 g $FeC_2O_4{\cdot}2H_2O$ and 1 mL of HCOOH were added to a 25 ml Teflon-lined stainless-steel autoclave, then, 1 mL of pyridine were added dropwise. The mixture was sealed and placed in an oven at 110 °C for 72 h without disturbance, then slowly cooled to room temperature at the rate of 2 °C/h. The black rod-shaped crystals of **1** were obtained with a yield of ~40% based on Fe.

$[HTHPM]_2[Fe^{III}Fe^{II}_2(HCOO)_7(C_2O_4)]$ (**2**): The synthesis of **2** is similar to that of **1**, except that 0.16 g $FeCl_3{\cdot}6H_2O$, 0.24 g $FeCl_2{\cdot}4H_2O$, 0.04 g $H_2C_2O_4{\cdot}2H_2O$, 2 ml of HCOOH and 1 ml of 1,3-propanediamine were used. The black rod-shaped crystals of **2** were obtained with a yield of ~40% based on Fe. 3,4,5,6-tetrahydropyrimidin-1-ium (THPM) cations was generated *in situ* by the reaction of 1,3-propanediamine with HCOOH.[S1]

$[HMPID]_2[Fe^{III}Fe^{II}_2(HCOO)_7(C_2O_4)$ (**3**): The synthesis of **3** is similar to that of **1**, except that 0.16 g $FeCl_3{\cdot}6H_2O$, 0.16 g $FeCl_2{\cdot}4H_2O$, 0.04 g $H_2C_2O_4{\cdot}2H_2O$, 1 ml of HCOOH and 1 ml of N-methylpyrrolidinamine were used. The black rod-shaped crystals are obtained. The estimated yield based on Fe is approximately 40%.

$[HPID]_2[Fe^{III}Fe^{II}_2(HCOO)_7(C_2O_4)]$ (**4**): The synthesis of **4** is similar to that of **1**, except that 0.16 g $FeCl_3{\cdot}6H_2O$, 0.16 g $FeCl_2{\cdot}4H_2O$, 0.04 g $H_2C_2O_4{\cdot}2H_2O$, 1.5 ml of HCOOH and 2 ml of pyrrolidinamine were used. The black rod-shaped crystals are obtained. The estimated yield based on Fe is approximately 40%.

Characterization Methods. The PXRD spectra were recorded on a rigaku D/Max-2500 diffractometer at 40kV, 100mA for a Cu-target tube and a graphite monochromator. Simulation of the PXRD spectrum was carried out by the Single-crystal data and diffraction-crystal module of the Mercury (Hg) program available free of charge via the internet at http://www.iucr.org. Magnetic susceptibility was measured by a Quantum Design MPMS superconducting quantum interference device (SQUID). Diamagnetic corrections were estimated by using Pascal constants and background corrections by experimental measurement on sample holders. Thermogravimetric (TGA) analyses were carried out on a Rigaku standard TG-DTA analyzer with a heating rate of 10°C min^{-1} from ambient temperature to 800°C under nitrogen gas. Differential scanning calorimetry (DSC) measurements were performed on a NETZSCH Analyzing under nitrogen at atmospheric pressure with a heating/cooling rate of 5 K min^{-1} for **2** and **3** but 5 K min^{-1} for **4**. Dielectric constant was measured with a Gwinstek LCR-meter over the frequency range of 500 Hz and 1 MHz at a heating/cooling rate of 2 K min^{-1} from 110 to 400 K. The temperature of the sample was controlled by the liquid nitrogen thermostat with an East changing TC280 Temperature Controller with uncertainty < 0.1 K.

X-ray Data Collection and Structure Determinations. The single-crystal X-ray diffraction data for **1**(273.15 K), **2**(379.98 and 293 K), **3**(292.69 and 400.15 K) and **4**(100, 299.17 and 370.15 K) were collected on a Rigaku SCXmini/XtaLAB AFC12/ Bruker D8 Venture single crystal X-ray diffractometer with Mo Kα radiation (λ = 0.71073 Å). The structure was determined directly by ShelXT and refined by full matrix least-squares methods using ShelXL with Olex2.[S2] It was further refined on F^2 with anisotropic thermal parameters. Hydrogen atoms were generated geometrically or from Fourier maps, and refined isotropically with fixed thermal factors. The detailed crystallographic data are listed in **Table S1**.

Table S1. Crystallographic Data for **1**, **2**, **3** and **4**.

Complexes	**1**	**2**LTP	**2**HTP	**3**LTP
Empirical formula	$C_{19}H_{19}Fe_3N_2O_{18}$	$C_{17}H_{25}Fe_3N_4O_{18}$	$C_{17}H_{25}Fe_3N_4O_{18}$	$C_{19}H_{31}Fe_3N_2O_{18}$
Formula weight	730.91	740.96	740.96	743.01
Temperature/K	273.15	293(2)	379.98(10)	292.69(18)
Crystal system	orthorhombic	orthorhombic	tetragonal	orthorhombic
Space group	$P2_12_12_1$	$P2_12_12_1$	$P\bar{4}2_1m$	$P2_12_12_1$
a/Å	11.973(2)	11.9937(9)	15.1110(12)	12.1064(8)
b/Å	14.917(3)	15.1397(9)	15.1110(12)	15.2095(13)
c/Å	15.127(3)	15.2063(11)	6.0078(7)	15.3444(10)
Volume/Å^3	2701.6(9)	2761.2(3)	1371.8(3)	2825.4(4)
Z	4	4	2	4
ρ(g/cm^3)	1.797	1.782	1.794	1.747
μ(MoKα)/mm^{-1}	1.677	1.643	1.654	1.604
F(000)	1476	1508	754	1524
Reflections collectec	4744	8714	7484	16106
Goodness-of-fit on F	1.103	0.983	1.077	1.052
Final R indexes [I≥2 (I)]	R_1 = 0.0387, wR_2 = 0.1028	R_1 = 0.0316, wR_2 = 0.0650	R_1 = 0.0383, wR_2 = 0.1004	R_1 = 0.0594, wR_2 = 0.1327
Final R indexes [all data]	R_1 = 0.0456, wR_2 = 0.1110	R_1 = 0.0760, wR_2 = 0.0828	R_1 = 0.0404, wR_2 = 0.1018	R_1 = 0.0786, wR_2 = 0.1433
Complexes	**3**HTP	**4**LTP	**4**ITP	**4**HTP
Empirical formula	$C_{19}H_{31}Fe_3N_2O_{18}$	$C_{17}H_{25}Fe_3N_2O_{18}$	$C_{17}H_{27}Fe_3N_2O_{18}$	$C_{17}H_{27}Fe_3N_2O_{18}$
Formula weight	743.01	712.94	714.95	714.95
Temperature/K	400.15(3)	100	299.17(10)	370.15
Crystal system	tetragonal	orthorhombic	orthorhombic	tetragonal
Space group	$P\bar{4}2_1m$	$P2_12_12_1$	*P*nma	*P*4/mbm
a/Å	15.2085(9)	11.804(2)	15.0662(11)	14.9876(15)
b/Å	15.2085(9)	14.956(2)	11.9292(7)	14.9876(15)
c/Å	6.0484(6)	14.961(3)	15.1536(10)	5.9643(9)

Volume/Å^3	1399.0(2)	2641.3(8)	2723.5(3)	1339.7(3)
Z	2	4	4	2
ρ(g/cm^3)	1.764	1.793	1.744	1.772
μ(MoKα)/mm^{-1}	1.620	1.712	1.661	1.688
F(000)	762	1452	1460	730
Reflections collected	15443	19026	14797	12503
Goodness-of-fit on F	1.051	1.030	1.173	1.080
Final R indexes [I≥2(I)]	R_1 = 0.0610, wR_2 = 0.1369	R_1 = 0.0501, wR_2 = 0.1245	R_1 = 0.0676, wR_2 = 0.1560	R_1 = 0.0648, wR_2 = 0.1730
Final R indexes [all data]	R_1 = 0.1123, wR_2 = 0.1682	R_1 = 0.0554, wR_2 = 0.1296	R_1 = 0.0959, wR_2 = 0.1695	R_1 = 0.0921, wR_2 = 0.2005

Table S2. The bonds lengths of **1**, **2**, **3** and **4** in LTP.

1LTP		**2**LTP		**3**LTP		**4**LTP	
Fe3-O1	2.184(5)	Fe3-O1	2.061(5)	Fe3-O1	2.191(6)	Fe3-O1	2.121(7)
Fe3-O2	2.131(5)	Fe3-O2	2.068(4)	Fe3-O2	2.149(7)	Fe3-O2	2.121(5)
Fe3-O5	2.114(5)	Fe3-O5	2.015(4)	Fe3-O5	2.078(7)	Fe3-O5	2.072(15)
Fe3-O13	2.035(5)	Fe3-O13	1.971(4)	Fe3-O13	2.116(7)	Fe3-O15	2.051(5)
Fe3-O15	2.102(5)	Fe3-O15	1.997(5)	Fe3-O15	2.090(6)	Fe3-O13	2.053(5)
Fe3-O17	2.153(5)	Fe3-O17	1.998(4)	Fe3-O17	2.102(7)	Fe3-O17	2.073(5)
Fe2-O3^{i}	2.061(5)	Fe2-O3^{i}	2.163(4)	Fe2-O3^{i}	2.101(8)	Fe2-O3^{i}	2.097(6)
Fe2-O4^{i}	2.043(5)	Fe2-O4^{i}	2.192(5)	Fe2-O4^{i}	2.073(7)	Fe2-O4^{i}	2.119(5)
Fe2-O6	2.011(5)	Fe2-O6	2.122(5)	Fe2-O6	2.054(6)	Fe2-O6	2.098(13)
Fe2-O7	1.970(5)	Fe2-O7	2.059(5)	Fe2-O7	2.049(6)	Fe2-O7	2.045(6)
Fe2-O11	1.982(5)	Fe2-O11	2.063(4)	Fe2-O11	2.044(7)	Fe2-O11	2.035(5)
Fe2-O18^{ii}	2.009(5)	Fe2-O18^{ii}	2.140(5)	Fe2-O18^{ii}	2.041(7)	Fe2-O18^{ii}	2.074(5)
Fe1-O8	2.146(6)	Fe1-O8	2.114(5)	Fe1-O8	2.084(7)	Fe1-O8	2.095(6)
Fe1-O9	2.116(6)	Fe1-O9	2.097(5)	Fe1-O9	2.069(6)	Fe1-O9	2.068(5)
Fe1-O10^{vi}	2.112(6)	Fe1-O10^{vi}	2.110(5)	Fe1-O10^{vi}	2.065(7)	Fe1-O10^{vi}	2.071(5)
Fe1-O12^{iii}	2.129(5)	Fe1-O12^{iii}	2.150(5)	Fe1-O12^{iii}	2.078(6)	Fe1-O12^{iii}	2.104(4)
Fe1-O14^{v}	2.091(6)	Fe1-O14^{v}	2.157(5)	Fe1-O14^{v}	2.076(7)	Fe1-O14^{v}	2.090(5)
Fe1-O16^{iv}	2.133(5)	Fe1-O16^{iv}	2.207(5)	Fe1-O16^{iv}	2.060(6)	Fe1-O16^{iv}	2.092(5)

Symmetry Code for **1**LTP, **3**LTP and **4**LTP:^{i}-1/2+x,1/2-y,3-z; ^{ii}-1+x,+y,+z; ^{iii}1/2-x,1-y,-1/2+z; ^{iv}-1/2+x,1/2-y,2-z; ^{v}1-x,-1/2+y,5/2-z; ^{vi}1/2+x,1/2-y,2-z.

Symmetry Code for **2**LTP: ^{i}-1/2+x,1/2-y,3-z; ^{ii}-1+x,+y,+z; ^{iii}1/2-x,1-y,1/2+z; ^{iv}-1/2+x,1/2-y,2-z; ^{v}1-x,-1/2+y,3/2-z; ^{vi}1/2+x,1/2-y,2-z.

Table 3. The bonds lengths of **2**HTP, **3**HTP, **4**ITP and **4**HTP.

2HTP		**3**HTP		**4**ITP		**4**HTP	
Fe1-O9^{vi}	2.094(14)	Fe1-O9^{vi}	2.033(14)	Fe1-O1	2.084(3)	Fe1-O1	2.048(6)
Fe1-O7	2.139(8)	Fe1-O7	2.033(14)	Fe1-O1^{i}	2.084(3)	Fe1-O1^{i}	2.048(6)
Fe1-O7^{iii}	2.139(8)	Fe1-O7^{iii}	2.033(14)	Fe1-O2	2.095(4)	Fe1-O1^{ii}	2.048(6)
Fe1-O8^{iv}	2.139(8)	Fe1-O8^{iv}	2.068(14)	Fe1-O2^{i}	2.095(4)	Fe1-O1^{iii}	2.048(6)
Fe1-O8^{ii}	2.128(8)	Fe1-O8^{ii}	2.069(14)	Fe1-O6^{ii}	2.101(4)	Fe1-O3^{i}	2.089(10)
Fe1-O10^{iii}	2.076(14)	Fe1-O10^{iii}	2.04(2)	Fe1-O6^{iii}	2.101(4)	Fe1-O3	2.089(10)
Fe2-O1	2.114(7)	Fe2-O1	2.085(16)	Fe2-O3	2.061(4)	Fe2-O2^{iv}	2.058(7)
Fe2-O3	2.078(7)	Fe2-O3	2.067(13)	Fe2-O4	2.068(4)	Fe2-O5	2.111(6)

Fe2-O5	2.008(7)	Fe2-O5	2.027(13)	Fe2-O5	2.052(4)	Fe2-O5^{iv}	2.111(6)
Fe2-O2^{i}	2.090(7)	Fe2-O2^{i}	2.150(16)	Fe2-O7	2.121(4)	Fe2-O4^{v}	2.083(7)
Fe2-O6^{i}	1.990(7)	Fe2-O6^{i}	2.083(13)	Fe2-O8^{iv}	2.139(4)	Fe2-O4^{vi}	2.083(7)
Fe2-O4^{v}	2.060(7)	Fe2-O4^{v}	2.044(14)	Fe2-O9	2.092(4)	Fe2-O2	2.058(7)

Symmetry Code for **2**HTP: ^{i} 1/2-y,1/2-x,+z; ^{ii} 1-x,1-y,+z; ^{iii} +y,1-x,1-z; ^{iv} 1-y,+x,1-z; ^{v} 1/2-y,1/2-x,1+z; ^{vi} 1-y,x,-z; **3**HTP: **3**HTP: ^{i} 1/2-y,1/2-x,+z; ^{ii} 1-x,1-y,+z; ^{iii} +y,1-x,1-z; ^{iv} 1-y,+x,1-z; ^{v} 1/2-y,1/2-x,1+z; ^{vi} 1-y,x,-z;. **4**ITP: ^{i}1-x,1-y,1-z; ^{ii}1/2-x,1-y,1/2+z; ^{iii}1/2+x,+y,1/2-z; ^{iv}1-x,1-y,-z. **4**HTP: ^{i} 1-x, 1-y, -1-z; ^{ii} y,1-x,-1-z; ^{iii}1-y, x, z; ^{iv}-1/2+y, 1/2+x,-1-z; ^{v}-1/2+y, 1/2+x, z; ^{vi} x, y, -1-z;

Table S4. The H-bonds lengths (Å) and angles (°) for **1**, **2, 3** and **4**.

Complex	D	H	A	d(D-H)/Å	d(H-A)/Å	d(D-A)/Å	D-H-A/°
1	N1	H1	O9^{vi}	0.86	2.01	2.864(17)	169.6
	N2	H2	O15^{ii}	0.86	1.93	2.760(10)	163.0
	N11	H11	O10^{vi}	0.86	2.04	2.904(18)	177.0
	Symmetry Code: ^{ii}-1+x,+y,+z; ^{vi}1/2+x,1/2-y,2-z;						
2LTP	N1	H1	O15	0.86	2.41	3.028(8)	129.5
	N1	H1	O16	0.86	2.33	3.183(8)	174.9
	N2	H2	O2 ^{vii}	0.86	2.69	3.218(8)	121.2
	N2	H2	O4^{vii}	0.86	2.19	2.993(9)	156.0
	N3	H3	O11	0.86	2.07	2.872(9)	155.2
	N4	H4	O9	0.86	2.54	3.226(9)	137.6
	N4	H4	O10	0.86	2.21	3.036(9)	162.1
	Symmetry Code: ^{vii}1-x,1/2+y,2/3-z;						
2HTP	N1	H1	O8	0.86	1.85	2.70(4)	170.5
	N2	H2	O1^{v}	0.86	2.28	2.94(3)	133.2
	N11	H11	O5	0.86	2.31	2.97(3)	133.9
	N22	H22	O1^{v}	0.86	2.17	2.98(4)	157.2
	Symmetry Code: ^{v} +y, 1-x,-z;						
3LTP	N1	H1	O1	0.98	2.08	2.94(4)	146.6
	N2	H2	O7^{vii}	0.98	2.19	2.99(3)	138.0
	N3	H3	O5^{viii}	0.98	2.27	3.10(3)	140.8
	N4	H4	O13	0.98	2.01	2.90(4)	150.1
	Symmetry Code: ^{vii} 1/2-x,1-y,1/2+z;^{viii} 1-x,1/2+y,5/2-z;						
3HTP	N1	H1	O2^{vii}	0.98	1.763	2.74(4)	174.38
	N2	H2	O6^{iv}	0.98	2.01	2.93(3)	154.27
	Symmetry Code: ^{iv} 1-y,+x,1-z; ^{vii} x, y,-1+z						
4LTP	N1	H1	O11	0.91	1.87	2.779(15)	174.5
	N1	H1	O13	0.91	1.91	2.820(18)	176.0
	N2	H2	O19^{v}	0.91	2.17	3.05(3)	163.1
	N2	H2	O13	0.91	1.91	2.820(18)	176.0
	N3	H3	O4	0.91	2.05	2.961(9)	175.4
	N3	H3	O7^{v}	0.91	2.11	2.961(10)	155.4
	Symmetry Code: ^{v} 1-x,-1/2+y,5/2-z;						
4(ITP)	N1	H1B	O3	0.89	2.19	3.04(4)	160.9

	N1	H1A	O8^{v}	0.89	2.29	3.16(4)	165.1
	N2	H2A	O3	0.89	2.11	2.94(3)	153.4
	N2	H2B	O8^{v}	0.89	2.15	3.02(3)	165.3
	N3	H3B	O5	0.89	1.98	2.865(12)	175.9
	N3	H3A	O5^{vi}	0.89	1.98	2.865(12)	175.9
	N4	H4B	O1^{viii}	0.89	2.42	3.10(2)	133.5
	N4	H4B	O1^{i}	0.89	2.42	3.10(2)	133.5
	N4	H4A	O9^{ii}	0.89	2.48	3.27(2)	148.4
	N4	H4A	O9^{vii}	0.89	2.48	3.27(2)	148.4
	^{i}1-x,1-y,1-z; ^{ii}1/2-x,1-y,1/2+z; ^{v}-1/2+x,+y,1/2-z;^{vi}+x,3/2-y,+z;^{vii}1/2-x,1/2+y,1/2+z;^{viii}1-x,1/2+y,1-z;						
	N1	H1a	O5	0.89	2.14	3.00(5)	159.97
4(HTP)	N1	H1b	O2^{vii}	0.89	2.311	3.09(5)	145.12
	Symmetry Code: ^{vii} y,1-x, z						

Table S5. The magnetic phase transition temperatures of some typical iron formates.

Topology	Complex	T_N/T_m (K)	Ref
$(4^{12}\cdot6^3)$	$[(CH_3)_2NH_2]Fe(HCOO)_3$	18	S3
	$[CH_3NH_2NH_2][Fe(HCOO)_3]$	21	S4
	$[CH_3NH_3]Fe(HCOO)_3$	17	S5
	$[NH_2CHNH_2][Fe(HCOO)_3]$	17.0	S6
	$[Fe(HCO_2)_3]_n\cdot{}_nHCO_2H$	20	S7
	$[C(NH_2)_3][Fe^{II}(HCOO)_3]$	10.0	S8
$(4^9\cdot6^6)$	$[NH_2NH_3][Fe(HCOO)_3]$	12.5	S9
	$[NH_4][Fe(HCOO)_3]$	9.4	S10
$(4^{12}\cdot6^3)$ $(4^9\cdot6^6)$	$[(CH_3)_2NH_2][Fe^{II}Fe^{III}(HCOO)_6]$	37	S11
	$[(C_2H_5)_2NH_2][Fe^{II}Fe^{III}(HCOO)_6]$	39	S12
	$[C_2H_5NH_3][Fe^{II}Fe^{III}(HCOO)_6]$	39	S12
	$[NH_3(CH_2)_4NH_3][Fe(HCOO)_3]_2$	19.8	S13
	$[CH_3NH_3][Fe^{III}Fe^{II}(HCO_2)_6]$	40	S14
$(4^{12}\cdot6^3)$ $(4^9\cdot6^6)_2$	$[(CH_3)_2NH_2]_2[Fe^{III}Fe^{II}{}_2(HCOO)_9]$	33	S15
	$[CH_3NH_2(CH_2)_2NH_2CH_3][Fe_2(HCOO)_6$	19.8	S16
	$[H_2meen\cdot H_2O][Fe^{III}(Fe^{II})_2(HCOO)_9]$	31.09	S17

	$[H_2dimeen][Fe^{III}(Fe^{II})_2(HCOO)_9]$	28.97	S17
	$[H_2dieten][Fe^{III}(Fe^{II})_2(HCOO)_9]$	25.67	S17
$(4^6{\cdot}5^3{\cdot}6)_2(4^8{\cdot}5^4{\cdot}6^3$	**1**	18	This work
	2	16	This work
	3	16	This work
	4	20	This work

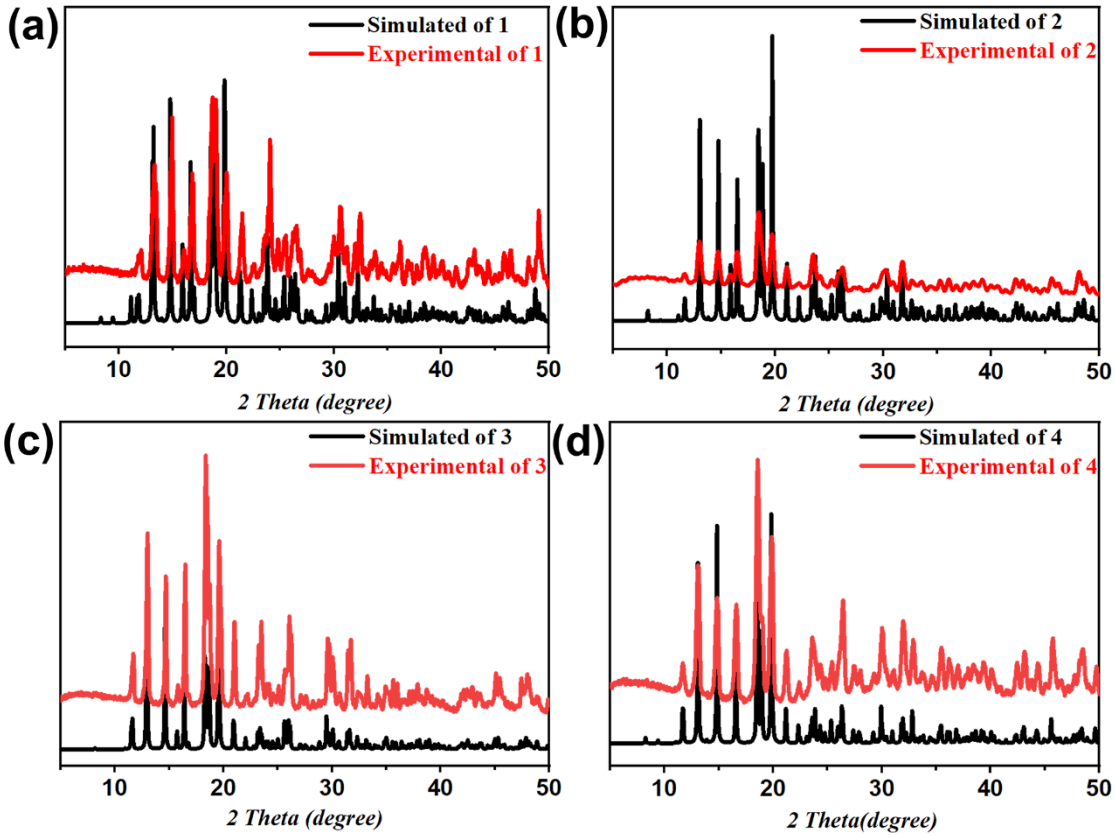

Figure S1. PXRD of **1**, **2**, **3** and **4**.

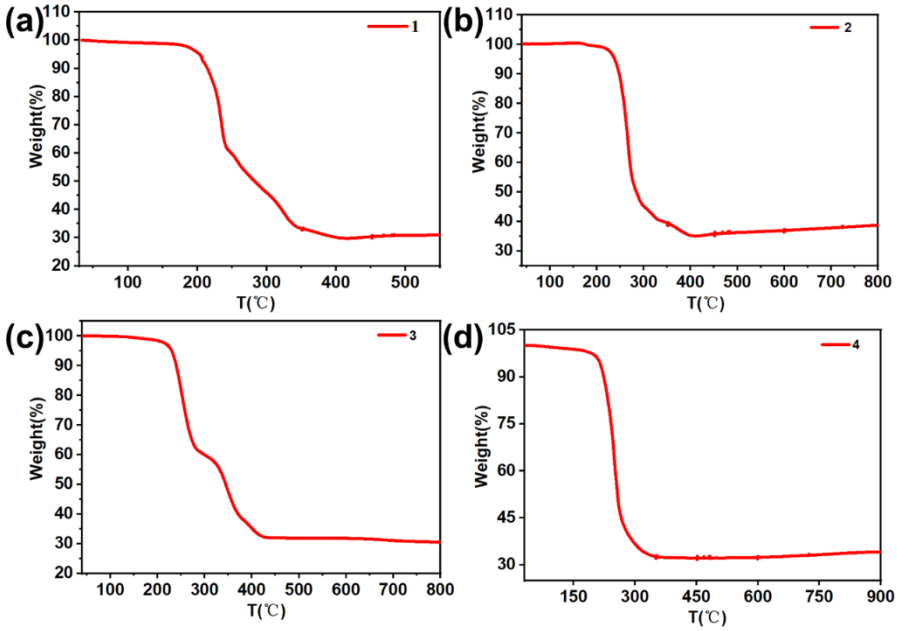

Figure S2. The TGA curves of **1**, **2**, **3** and **4** with the heating rate of 10 K min^{-1} under N_2 atmosphere.

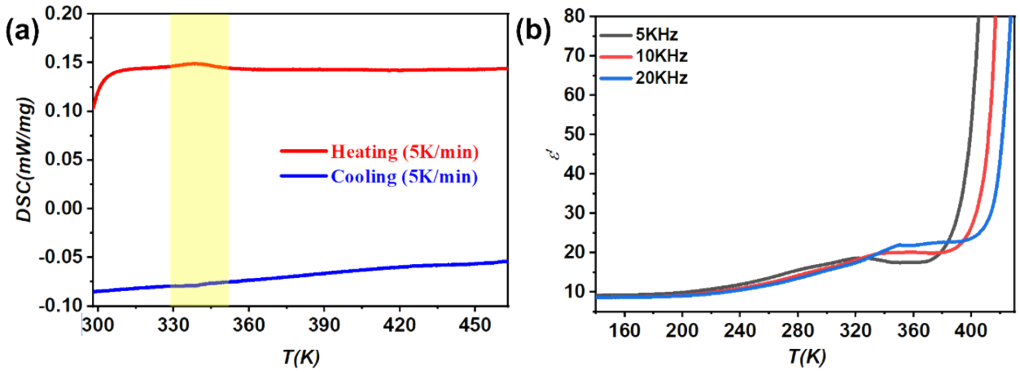

Figure S3. (a) DSC curves of **3** in the heating–cooling cycle. (b) Real dielectric part of the constant (ε') of **3** measured at 5 kHz, 10 kHz and 20 kHz upon the heating process.

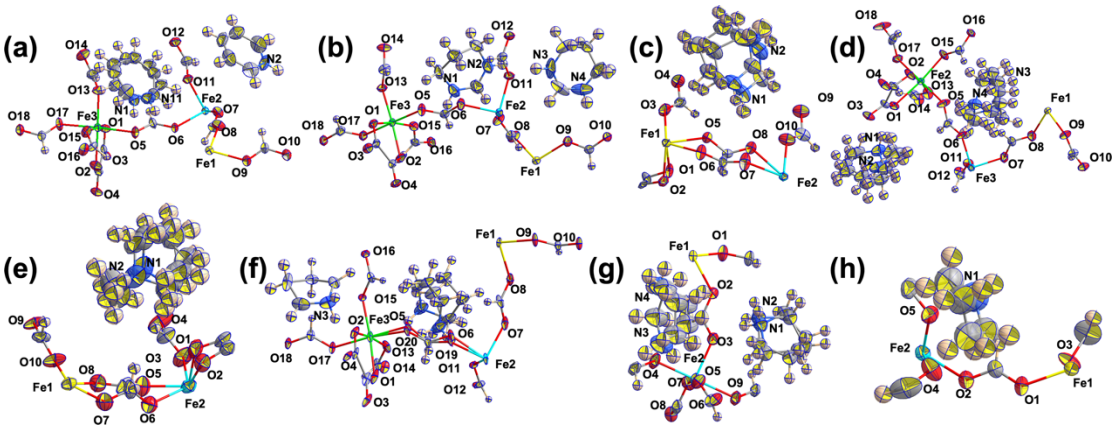

Figure S4. (a)-(h) the ellipsoid (50 % for C, N, Fe, O and 20% for H) plot of atoms in the asymmetric unit for **1**, **2**LTP, **2**HTP, **3**LTP, **3**HTP, **4**LTP, **4**ITP and **4**HTP.

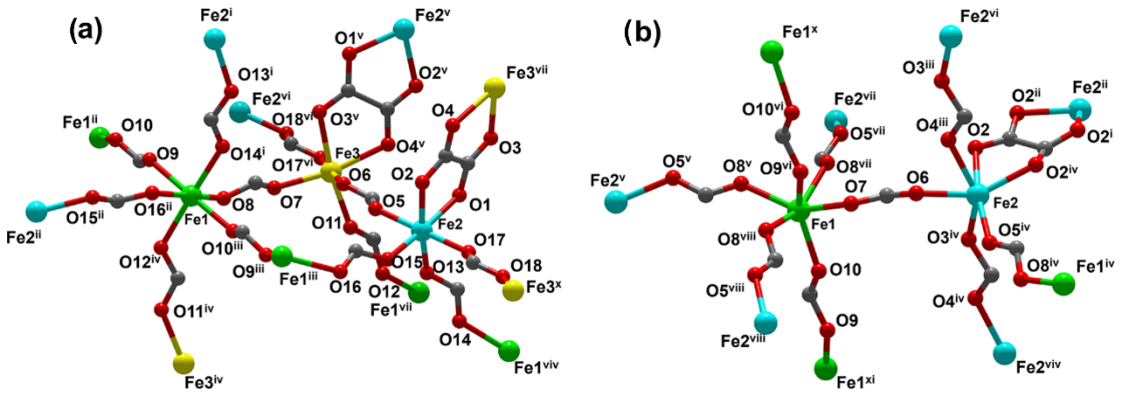

Figure S5. (a) Coordination mode diagrams of crystals **2** in LTP: green, blue, yellow, red and grey spheres represent Fe1, Fe2, Fe3, O and C atoms, respectively. H atoms are omitted for clarity. Symmetry codes: [i]1-x, -1/2+y, 5/2-z; [ii]-1/2+x, 1/2-y, 2-z; [iii]1/2+x, 1/2-y, 2-z; [iv]1/2-x, 1-y, -1/2+z; [v]-1/2+x, 1/2-y, 3-z; [vi]-1+x,+y,+z; [vii]1/2-x, 1-y, 1/2+z; [viii]1/2+x, 1/2-y, 3-z; [viv]1-x, 1/2+y, 5/2-z; [x]1+x, +y, +z. (b) Coordination mode diagrams of crystals **2** in HTP: green, blue, red and grey spheres represent Fe1, Fe2, O and C atoms, respectively. Symmetry codes: [i]1-x, -y, +z; [ii]-1/2+x, 1/2+y, +z; [iii]1/2-x, 1/2-y, 1+z; [iv]1/2-x, 1/2-y, +z; [v]1-x, 1-y, +z; [vi]+x,+y,1+z; [vii]+x, 1-y, 1-z; [viii]1-x, +y, 1-z; [viv]+x, +y, -1+z; [x]1-x, 1-y, 1+z; [xi]1-x, +y, -z.

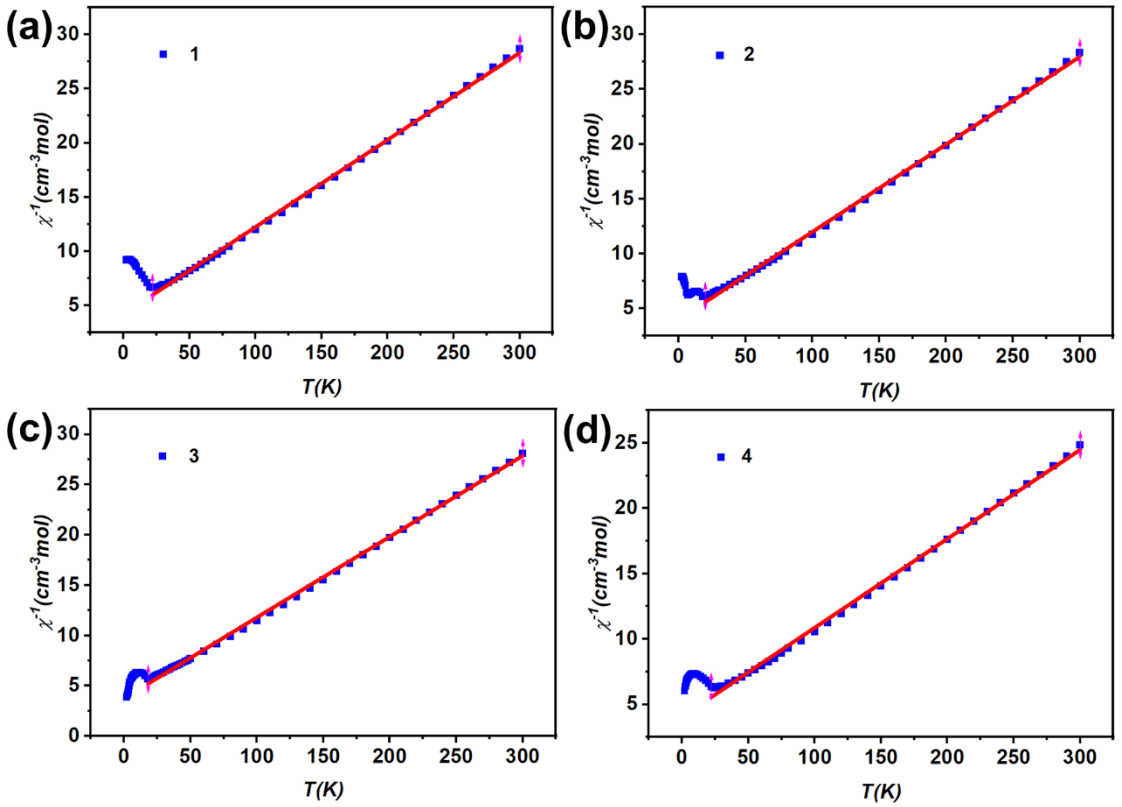

Figure S6. The Curie-Weiss fitting of **1**, **2**, **3** and **4**.

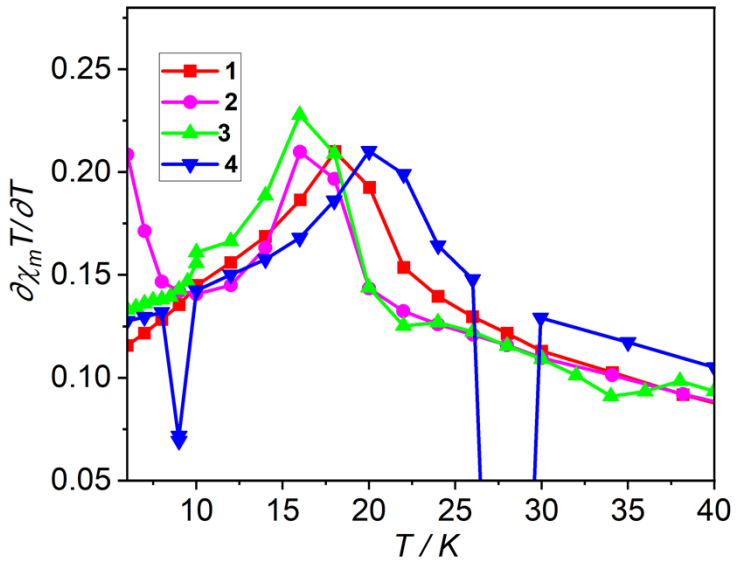

Figure S7. The derivative curve of $\chi_m T$ *vs* T plots at low temperature.

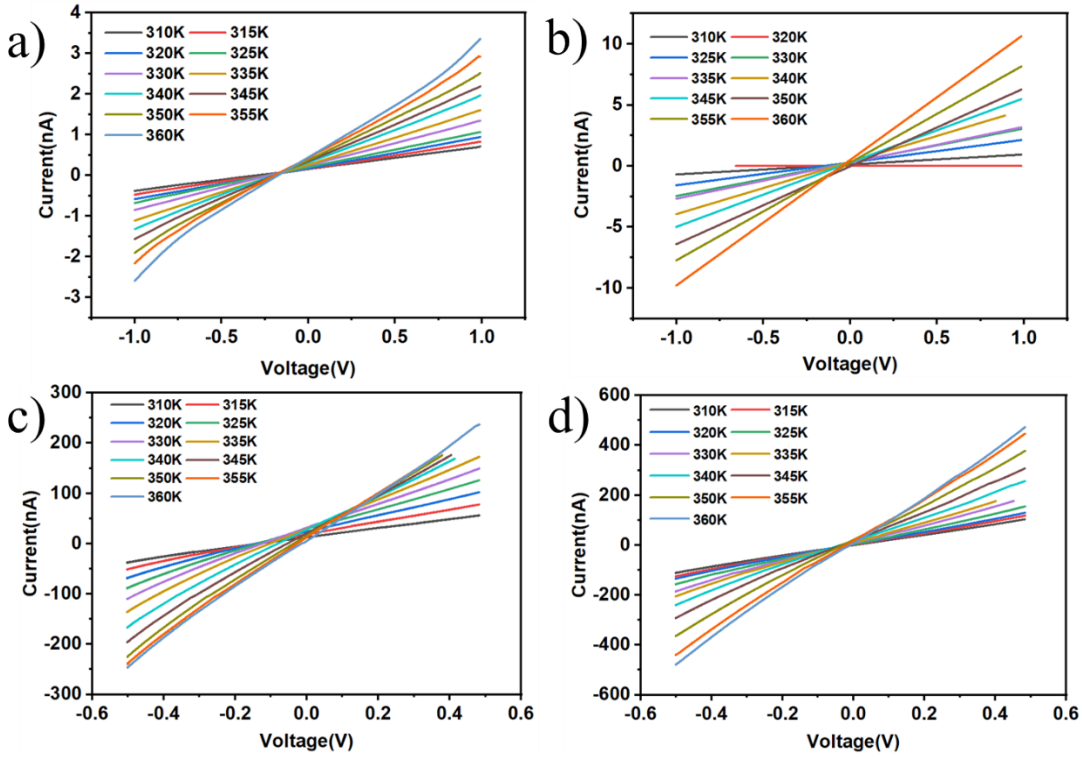

Figure S8 a)-d) Voltage-current curves at different temperatures of **1**-**4**.

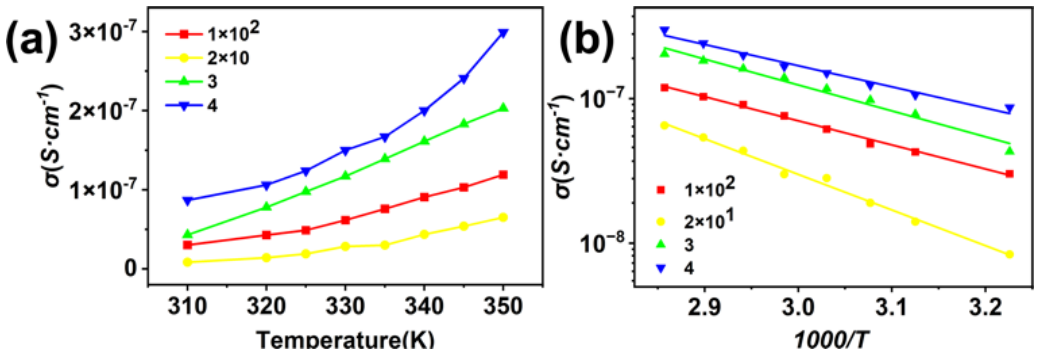

Figure S9. a) Variable-temperature conductivity measurement of 1-4. b) The logarithmic plots of the temperature-dependent conductivity versus 1000/T of 1-4, where the solid line represents the Arrhenius fitting.

References:

S1. G.-H. Ni, Y.-X. Sun, C.-X. Ji, Y.-W. Jin, M.-Y. Liu, J.-P. Zhao and F.-C. Liu,. *Cryst. Growth Des.*, 2022, **22**, 3428−3434.

S2. (a) G. M. Sheldrick, Acta Crystallogr. Sect. *C-Struct. Chem.*, 2015, **71**, 3-8. (b) W. A. Paciorek, M. Meyer and G. Chapuis, *Acta Crystallogr. Sect. A*, 1999, **55**, 543-557. (c) L. J. Bourhis, O. V. Dolomanov, R. J. Gildea, J. A. Howard and H. Puschmann, *Acta Crystallogr. Sect. A*, 2015, **71**, 59-75.

S3. Y. Tian, J. Cong, S. Shen, Y. Chai, L. Yan, S. Wang and Y. Sun, *Phys. Status Solidi RRL*, 2014, **8**, 91.

S4. M. Mączka, A. Gągor, M. Ptak, W. Paraguassu, T. A. de Silva, A. Sieradzki and A. Pikul, *Chem. Mater.*, 2017, **29**, 2264.

S5. L. Cañadillas-Delgado, L. Mazzuca, S. Ling, M. J. Cliffe and O. Fabelo, *Inorg. Chem.*, 2025, **64**, 7348.

S6. A. Ciupa, M. Mączka, A. Gągor, A. Pikul, E. Kucharska, J. Hanuza and A. Sieradzki, *Polyhedron*, 2015, **85**, 137.

S7. V. Paredes-García, I. Rojas, R. Madrid, A. Vega, E. Navarro-Moratalla, W. Cañón-Mancisidor, E. Spodine and D. Venegas-Yazigi, *New J. Chem.*, 2013, **37**, 2120.

S8. K.-L. Hu, M. Kurmoo Dr, Z. Wang and S. Gao, *Chem. Eur. J.*, 2009, **15**, 12050.

S9. M. MąCZKA, K. Pasińska, M. Ptak, W. Paraguassu, T. A. D. Silva, A. Sieradzki and A. Pikul, *Phys. Chem. Chem., Phys.*, 2016, **18**, 31653.

S10. G.-C. Xu, W. Zhang, X.-M. Ma, Y.-H. Chen, L. Zhang, H.-L. Cai, Z.-M. Wang, R.-G. Xiong and S. Gao, *J. Am. Chem. Soc.*, 2011, **133**, 14948.

S11. K. Hagen, S. G. Naik, B. H. Huynh, A. Masello and G. Christou, *J. Am. Chem. Soc.*, 2009, **131**, 7516.

S12. M. MąCZKA, A. Ciupa, A. Gągor, A. Sieradzki, A. Pikul and M. Ptak, *J. Mater. Chem. C*, 2016, **4**, 1186.

S13. R. Shang, S. Chen, K.-L. Hu, B.-W. Wang, Z.-M. Wang and S. Gao, *Chem. Eur. J.*, 2016, **22**, 6199.

S14. J. Zhao, W. Wang, S. Han, Q. Li, N. Li, F. Liu and X. Bu, *Acta Chim. Sinica*, 2020, **78**, 1223.

S15. K.-H. Jin, S.-Y. Wang, K. Wang, B. Xia, Y.-Z. Tong, Y. Ma and Q.-L. Wang, *Inorg. Chem. Comm.*, 2019, **105**, 26.

S16. M.-Y. Li, M. Kurmoo, Z.-M. Wang and S. Gao, *Chem. Asian J.*, 2011, **6** ,3084.

S17. Q.-Y. Yan, S. D. Han, T. Xu, C.-X. Ji, L.-L. Lv, Z.-Q. Yao, J.-P. Zhao and F.-C. Liu, *Chem. Commun.*, 2025, **61**, 16412.